

Cite this: *J. Mater. Chem. A*, 2018, 6, 15095Received 23rd May 2018  
Accepted 2nd July 2018

DOI: 10.1039/c8ta04817g

rsc.li/materials-a

# Anthraquinone thin-film electrodes for reversible CO<sub>2</sub> capture and release†

Dominik Wielend,<sup>ID</sup>\* Dogukan Hazar Apaydin<sup>ID</sup> and Niyazi Serdar Sariciftci<sup>ID</sup>

We report reversible electrochemical capture and release of carbon dioxide using the well-known dye precursor and industrial catalyst anthraquinone. Although quinones are well-studied for electrochemical capture and release of CO<sub>2</sub> in solution, we have discovered that a 100 nm film of anthraquinone can realize this in a heterogeneous fashion. In-depth spectroelectrochemical studies were performed in order to study the mechanism of this CO<sub>2</sub> capture and release. Anthraquinone films reached an uptake capacity of 5.9 mmol<sub>CO<sub>2</sub></sub> g<sub>AQ</sub><sup>-1</sup>.

## 1. Introduction

The general strategy of Carbon Capture and Utilization (CCU) aims to use and recycle carbon dioxide (CO<sub>2</sub>) towards useful chemicals. Several approaches have been emerging in the scientific community during the last decades to realize this strategy.<sup>1–5</sup> Before reducing CO<sub>2</sub> one has to capture and concentrate carbon dioxide from the atmospheric contents of 400 ppm. In addition to the use of industrial capture methods<sup>6</sup> like amine scrubbing,<sup>7,8</sup> organic solvents<sup>9</sup> or physical adsorption on high surface-area materials<sup>10,11</sup> the electrochemical capture and release of carbon dioxide offers interesting possibilities.

A promising class of materials for electrochemical CO<sub>2</sub> capture is the carbonyl bearing conjugated compound family. In 1984 Harada *et al.* reported unsaturated  $\alpha,\beta$ -ketones for carboxylation upon electrochemical reduction.<sup>12</sup> Some years later quinones became well-studied in homogeneous solutions for CO<sub>2</sub> capture upon the formation of electrogenerated nucleophiles while forming carbonate-like structures.<sup>13–16</sup> A very recent publication by Yin *et al.* describes the application of quinones, including anthraquinone, as mediators in lithium–CO<sub>2</sub> batteries.<sup>17</sup> Recent publications by our group investigated thin films of carbonyl pigments (quinacridone and a naphthalene bisimide derivative, NBIT) for heterogeneous electrochemical capture and release.<sup>18,19</sup>

Besides carbonyl compounds also electrochemically activated 4,4'-bipyridinium<sup>20,21</sup> and recently benzyldisulfide<sup>22</sup> compounds were reported to reversibly capture and release of carbon dioxide in organic solvents and ionic liquids. Furthermore, Liu and Landskron reported supercapacitive swing

absorption, an energy-efficient way, for CO<sub>2</sub> capture and release.<sup>23</sup>

Most of these systems reported in literature are either operated in organic solvents,<sup>12–14,18,20</sup> ionic liquids<sup>15,16,21,22</sup> or contain specially synthesized tailor-made compounds.<sup>19</sup> An industrially-scalable, cheap and abundant chemical compound which can take up the task is still missing. In this work, we demonstrate that the infamous, simple compound, anthraquinone is up to the task and capable of electrochemical capture and release carbon dioxide efficiently.

## 2. Experimental

### Electrode preparation

Glassy carbon electrodes at a size of 4 × 1 cm were initially cleaned with 18 M $\Omega$  water (MQ) and acetone (VWR Chemicals, technical grade). Afterwards each side was polished for 30 s with a Buehler Micropolish II deagglomerated alumina in decreasing particle sizes from 1.0 to 0.3 to 0.05  $\mu$ m. Cleaning in between was performed by sonication in iso-propanol (VWR Chemicals, AnalaR Normapur) and MQ water. In a last step, excess Al<sub>2</sub>O<sub>3</sub> was removed by polishing each side for 30 s with toothpaste followed by sonication in iso-propanol and MQ water.

The final step was electrochemical cleaning by sweeping the potential between +1.5 and –1.0 V vs. Ag/AgCl/3 M KCl in 0.5 M H<sub>2</sub>SO<sub>4</sub> at a speed of 50 mV s<sup>-1</sup> for 30 cycles.

Glass (0.7 × 6.0 cm) and FTO/glass (0.75 × 2.5 cm) substrates were cut into the appropriate size followed by cleaning *via* sonication for 30 min each in the following media: acetone (VWR chemicals, technical grade), 2% Hellmanex solution (Hellma-Analytics), MQ water and iso-propanol (VWR Chemicals, AnalaR Normapur).

Glass samples are further treated in an evaporation chamber for thermal evaporation of 5 nm chromium followed by 80 nm of gold.

Linz Institute for Organic Solar Cells (LIOS), Institute of Physical Chemistry, Johannes Kepler University Linz, Altenbergerstrasse 69, 4040 Linz, Austria. E-mail: dominik.wielend@jku.at

† Electronic supplementary information (ESI) available. See DOI: 10.1039/c8ta04817g



### Anthraquinone evaporation

1.0 g of commercially-available anthraquinone (Sigma Aldrich, 97%) were purified by sublimation at 250 °C under vacuum for 20 h. This product from 2 batches was purified following this protocol a second time before using it in an organic material evaporator. Evaporation was performed at 57 °C at  $\sim 10^{-6}$  mbar for 50 s. Under those conditions uniform AQ films with a thickness of 100 nm were formed. The average thickness and evaporation speed in  $\text{nm min}^{-1}$  respectively was determined by a Bruker DekTak XT Profilometer.

### Electrochemistry

For electrochemical characterization experiments a Jaislle Potentiostat-Galvanostat 1030 PC-T was used. For simple cyclic voltammetry (CV) experiments a two-compartment cell containing a three-electrode setup was used. 20.0 mL of 0.1 M  $\text{Na}_2\text{SO}_4$  solution was used as electrolyte solution. A platinum electrode was used as counter electrode (CE), a commercial Ag/AgCl/3 M KCl electrode as reference electrode (RE) and a 100 nm film of AQ on either Cr-Au/glass or glassy carbon as working electrode (WE).

The cell was purged with nitrogen gas ( $\text{N}_2$ ) for one hour prior to electrochemical measurements. After CV measurement, the cell was purged one hour with carbon dioxide ( $\text{CO}_2$ ). To remove  $\text{CO}_2$  again from the electrolyte solution, another two hours purging with  $\text{N}_2$  was applied.

In all CV measurements two cycles were recorded and due to reason of reproducibility always the second cycles were plotted.

### UV-vis spectroelectrochemistry

For UV-vis spectroelectrochemistry a quartz cuvette filled with 2 mL of 0.1 M  $\text{Na}_2\text{SO}_4$  electrolyte solution was used. An Ag/AgCl wire was utilized as quasi reference electrode, a platinum wire as CE and an AQ/FTO/glass as WE. A Jasco V-670 Spectrophotometer was used for performing the absorption experiments.

One absorption measurement took 20 s which is the reason for setting step potentials in 0.1 V steps changing every 20 s. Starting from 0.0 V the potential was decreased gradually to  $-1.8$  V (all vs. Ag/AgCl).

Under  $\text{N}_2$  conditions the final vial setup was purged with  $\text{N}_2$  for 45 min. Under  $\text{CO}_2$  conditions after purging 45 min with  $\text{N}_2$ , another 45 min purging with  $\text{CO}_2$  was performed.

### FTIR spectroscopy

For ATR-FTIR spectroelectrochemistry an AQ/Ge crystal was used as WE whereas standard Ag/AgCl wire is used as RE and a platinum plate as CE. A constant flow of  $3 \text{ mL min}^{-1}$  of 0.1 M  $\text{Na}_2\text{SO}_4$  electrolyte solution was established and the same step potential as in UV-vis spectroelectrochemistry was applied. In those experiments potentials up to  $-2.1$  V vs. Ag/AgCl were applied.

A bottle of the electrolyte solution was purged with  $\text{N}_2$  over night. A fraction of it was taken out and in a separate bottle in addition purged with  $\text{CO}_2$  again for one night.

The ATR-FTIR *in situ* spectroelectrochemistry studies were performed on a Bruker IFS-66/S machine averaging over 32 scans. The ATR-FTIR spectra of pure anthracene and anthraquinone were recorded on a Bruker Vertex 80-ATR machine.

The mentioned *in situ* spectroelectrochemical investigations were performed one time under  $\text{N}_2$  and once  $\text{CO}_2$  conditions.

For the  $\text{CO}_2$  capture/release quantification a one-compartment cell with a total volume of 23.3 mL was used. An AQ/Cr-Au/glass electrode acted as WE, an Ag/AgCl as RE and a platinum wire as CE. 13.3 mL of 0.1  $\text{Na}_2\text{SO}_4$  as electrolyte solution were used resulting in a total free headspace of 10.0 mL.

After purging the cell for 1 h with  $\text{N}_2$  and 1 h with  $\text{CO}_2$ , two CV cycles for capturing were performed. After removing the excess  $\text{CO}_2$  by 2 h purging with  $\text{N}_2$  again two CV cycles for release were performed. Afterwards a 2 mL aliquot of the headspace is taken and injected into a  $\text{N}_2$  purged IR gas cell. Measuring of the FTIR spectrum and integration of the area in absorbance mode allows quantification of the released amount of  $\text{CO}_2$ .

A calibration curve was made by injection of defined aliquots of a 5%  $\text{CO}_2$  in  $\text{N}_2$  mixture into the  $\text{N}_2$  flushed IR gas cell. After equilibration of the conditions for 45 min in the Bruker IFS-66/S machine to remove  $\text{CO}_2$  from the machine, IR spectra were recorded and integrated and the calibration curve was obtained (see ESI Fig. S1†).

## 3. Results and discussion

The first step to examine the application of the industrial dye precursor anthraquinone (AQ) as potential electrochemical carbon dioxide capture agent was performing cyclic voltammetry (CV) at different conditions. Thermally evaporated films of anthraquinone with an optimized thickness of 100 nm in aqueous 0.1 M  $\text{Na}_2\text{SO}_4$  solution exhibited promising electrochemical behavior upon CV measurement as shown in Fig. 1.

The initial nitrogen ( $\text{N}_2$ ) saturated conditions in Fig. 1 show a quasi-reversible reduction feature at  $-0.80$  V which is in accordance to homogenous reduction of anthracene-9,10-diol (hydroquinone) structure reported in literature.<sup>24-26</sup> Under  $\text{CO}_2$  saturated conditions the electrochemical response of AQ nearly vanished and only very low current was observed upon further reduction.

After removal of unbound  $\text{CO}_2$  out of the system and saturation of the solution with  $\text{N}_2$  followed by electrochemical oxidation gave rise to a small oxidation peak at  $+0.27$  V which was assigned to the release of carbon dioxide. Afterwards, cycling further to negative potentials reveals once more characteristic quasi-reversible reductive feature of AQ. The significant decrease in current density from initial  $-0.68$  to  $-0.22 \text{ mA cm}^{-2}$  after release could be explained by the dissolution of the soluble hydroquinone species from the electrode.

The vanishing of the reductive peaks behavior was already reported for different carbonyl bearing pigments in literature.<sup>18,19</sup> Like in the previous system we assigned this to the *in situ* formation of a carbonate-like structure illustrated in Fig. 1.



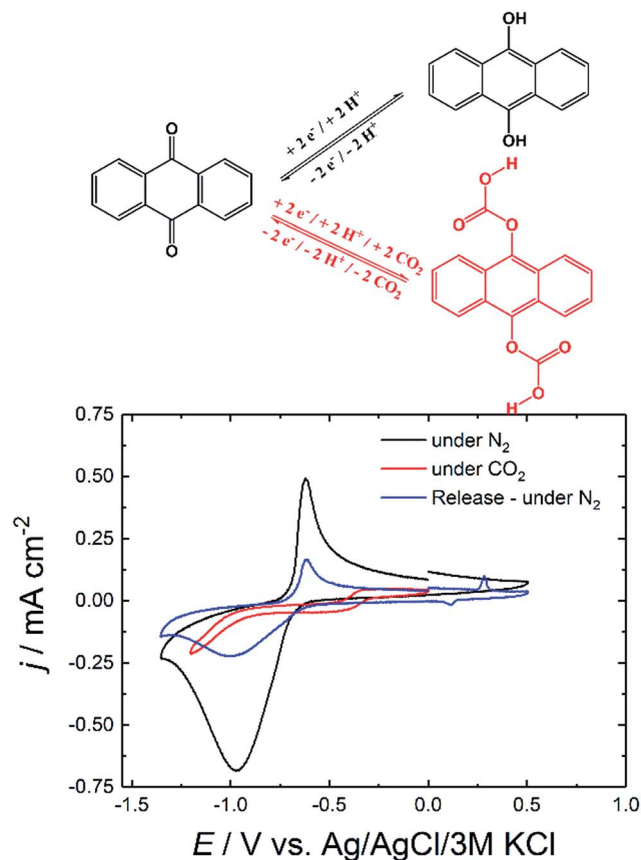


Fig. 1 CV curves of AQ on glassy carbon (GC) under different gas-saturated conditions.

In further experiments not only glassy carbon was used as electrode material but also thin-layers of chromium and gold (Cr–Au) on glass substrates. The CV of AQ/Cr–Au/glass is shown in Fig. 2 in order to confirm the similarity to the CV of AQ/glassy

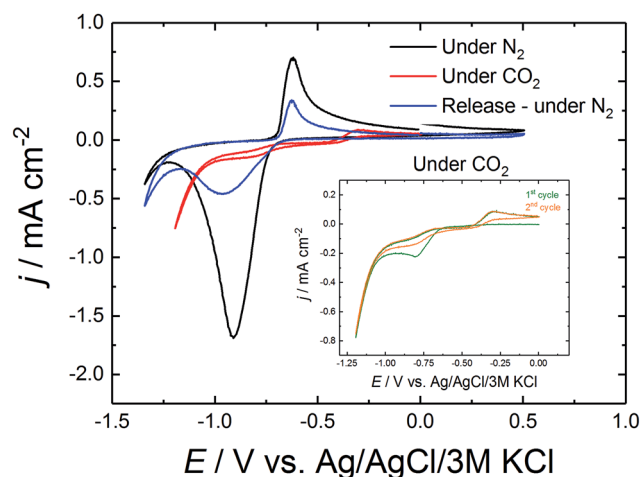


Fig. 2 Cyclic voltammetry of AQ/Cr–Au/glass in 0.1 M Na<sub>2</sub>SO<sub>4</sub>. The insert shows the comparison of the first and the second cycle of CV under CO<sub>2</sub>.

carbon. Furthermore, the comparison of the first and the second cycle under CO<sub>2</sub> is shown in the same graph.

Comparing the curves of AQ/Cr–Au in Fig. 2 to the ones of AQ/GC in Fig. 1 revealed a nearly identical shape. The only difference was the lack of the small oxidative release peak at +0.27 V. To the best of our knowledge, this might be due to the fact that glassy carbon possesses a different surface structure than gold. We observe, that on gold a rearrangement of the AQ was taking place which caused the lack of this peak (Fig. 3).

As discussed before, initially the AQ is reduced forming nucleophilic hydroquinone structure which is then presumed to bind CO<sub>2</sub>.<sup>13,14,16</sup> This theory was supported by comparing the first CV cycle under CO<sub>2</sub> with the second one in the inset of Fig. 2. The first cycle still showed the reductive peak of anthraquinone, which in the second cycle disappeared due the formation of the mentioned carbonate-like structure. Under those CO<sub>2</sub> conditions, this flat CV behavior was observed over 50 cycles. Only after repurging the system with N<sub>2</sub> and releasing CO<sub>2</sub> by sweeping to the oxidative side, the reductive peak of anthraquinone was recovered again.

We have also observed physical changes on the crystal structure of AQ thin films. Fig. 3 shows SEM image of AQ film directly after evaporation (on the left) forming a quite uniform brick-like structure. Upon performing the electrochemical capture and release of carbon dioxide, needle-like microcrystals (Mikado-like) were observed (on the right).

Such recrystallization of carbonyl pigments has also already been reported.<sup>27,28</sup> The reason for this was most probably the partial dissolving and recrystallization of AQ molecules during the process.

To further investigate and characterize the optical absorption changes, UV-vis spectroelectrochemistry experiments were conducted as shown in Fig. 4.

The pictures A to D in Fig. 4 show the observed color changes upon electrochemistry on a Cr–Au electrode. Under electrochemical reduction under N<sub>2</sub> saturated conditions (Fig. 4B and D) a color change to red-orange caused by the soluble anthracene-9,10-diol species was observed. Besides, under CO<sub>2</sub>-rich atmosphere (Fig. 4C) no dissolving process but a change to a brighter yellow species was observed.

These qualitative observations were justified by the UV-vis spectroelectrochemistry. Under N<sub>2</sub> saturated conditions three strong absorption bands at 390, 416 and 460 nm were observed. According to Babaei *et al.* and Shamsipur *et al.* the three bands could be correlated to differently protonated anthracene-9,10-diol species whereas in this aqueous surrounding the presence of a radical species was very unlikely.<sup>25,26</sup> The absorption maximum for AQ<sup>2-</sup> was reported at 466/470 nm and the one for AQH<sup>-</sup> at 412/414 nm. As they reported that protonation was causing a blueshift in absorption, the detected band at 390 nm could be assigned to the AQH<sub>2</sub> species.<sup>25,26</sup>

In contrast, under CO<sub>2</sub> saturated conditions the system was forming an absorption shoulder at 440 nm which was responsible for the brighter yellow color shown in Fig. 4C. To further substantiate the proposed anthraquinone–carbonate structure depicted in Fig. 1, *in situ* ATR-FTIR spectroelectrochemistry of AQ on a germanium (Ge) reflection element/electrode was



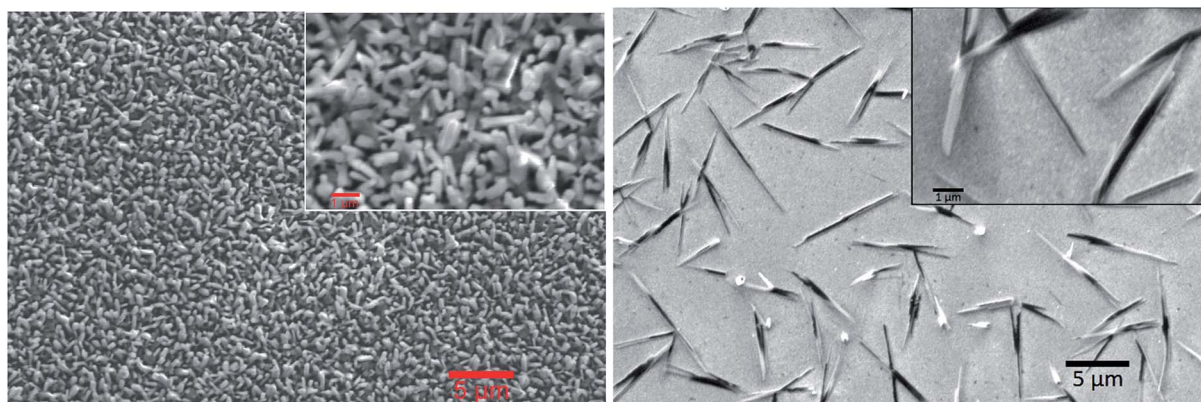


Fig. 3 Scanning electron microscopy (SEM) images of the pristine anthraquinone film on Cr–Au on glass (left) and after electrochemical CO<sub>2</sub> capture and release (right).

conducted under CO<sub>2</sub> conditions (N<sub>2</sub> conditions shown in Fig. S2†). In Fig. 5 the characteristic region is zoomed in and the arising/disappearing bands were correlated with the molecular structural changes.

In analogy to the IR spectrum under N<sub>2</sub> saturated conditions (see ESI†) quite strong negative bands (disappearing of functional groups) were observed upon reductive dissolving of anthraquinone shown in Fig. 5. In order to compare the disappearing peaks with the material, ATR-IR powder spectra of anthracene and anthraquinone were measured, shown in Fig. 6.

According to the ATR-IR powder spectra of anthraquinone and anthracene in Fig. 6 and from the examples in literature<sup>29</sup>

the disappearing peaks could fully be correlated to anthraquinone and the characteristic C=O bands, respectively.

The fluctuations in the baseline of the measurements might arise from the air that is trapped within the powder.

The arising band at 1066 cm<sup>-1</sup> under N<sub>2</sub> conditions was a proof for C<sub>arom</sub>-O stretching vibration in the anthracene-9,10-diol structure.<sup>30</sup> Under CO<sub>2</sub> conditions two bands at 1051/1018 cm<sup>-1</sup> indicated the formation of C<sub>arom</sub>-O single bonds.<sup>30</sup> As those bands appeared at lower frequencies compared to nitrogen conditions, they were assumed to be caused by larger moieties attached to the oxygen atom. Also, a literature report from Criswell and Klanderman assigned bands in this wave-number region from 960 to 1060 cm<sup>-1</sup> to C–O bonds in

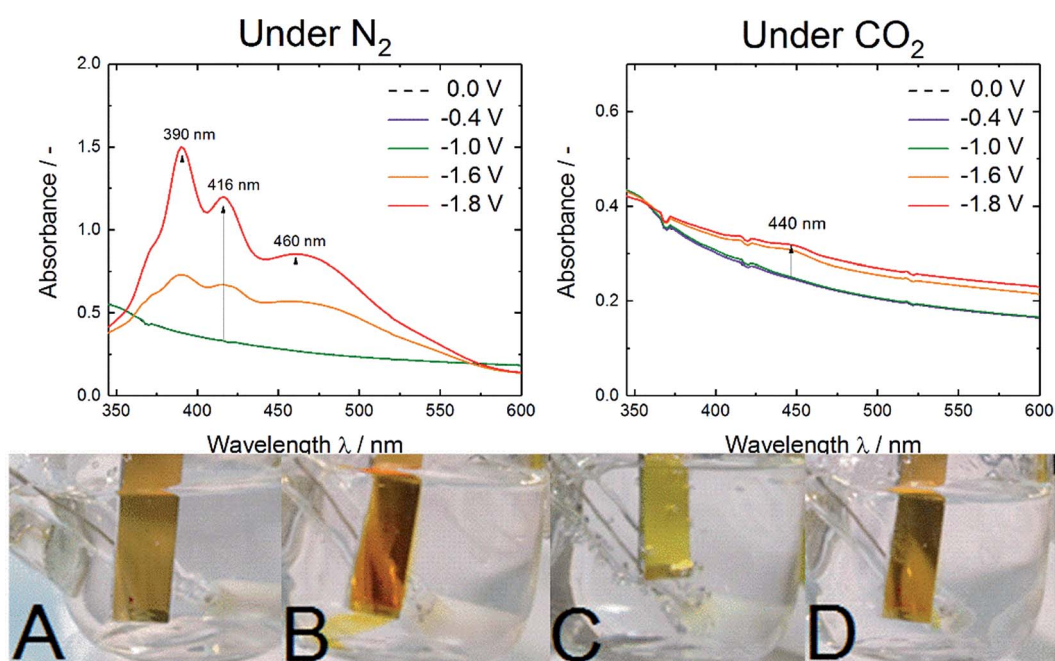


Fig. 4 UV-vis spectra of AQ/FTO/glass electrodes under nitrogen saturated conditions (left) and under CO<sub>2</sub> saturated conditions (right) at various potentials vs. Ag/AgCl. On the bottom pictures of AQ/Cr–Au/glass while performing CV are shown. (A) No potential applied, (B) at –1.0 V vs. Ag/AgCl/3 M KCl under N<sub>2</sub>, (C) at –1.0 V vs. Ag/AgCl/3 M KCl under CO<sub>2</sub>, (D) at –1.0 V vs. Ag/AgCl/3 M KCl after release under N<sub>2</sub>.



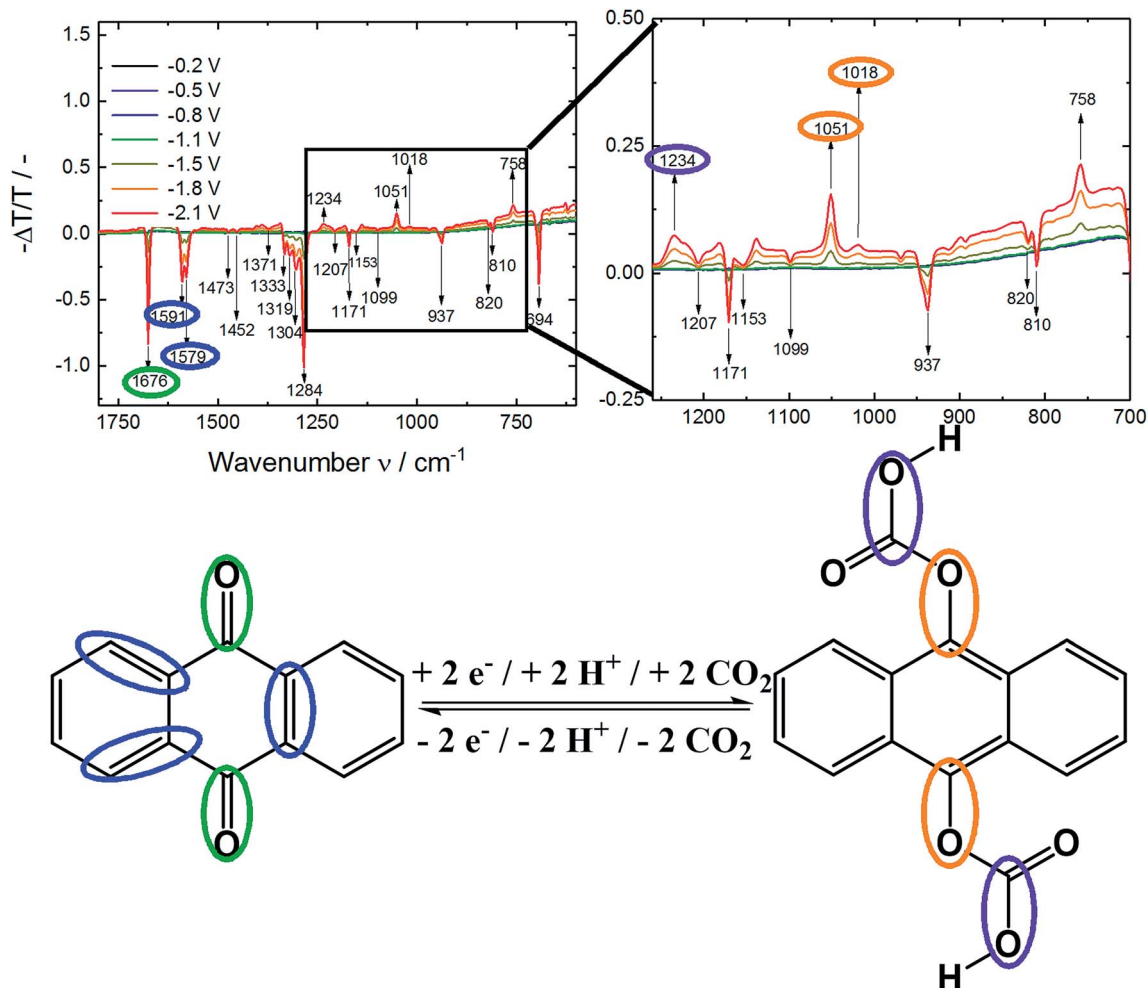


Fig. 5 ATR-FTIR spectroelectrochemistry of AQ/Ge under CO<sub>2</sub> saturated conditions at various potentials vs. Ag/AgCl (top). On the bottom the proposed structure of the anthraquinone-carboxylic acid species with assignment of functional groups to the IR spectrum.

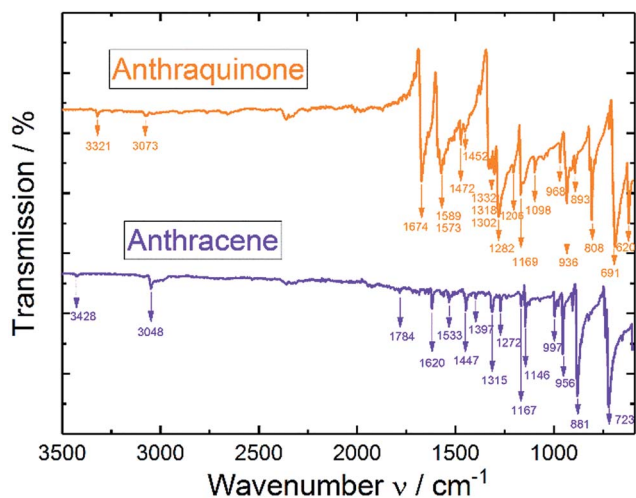


Fig. 6 ATR-IR spectra of pure anthracene and anthraquinone powders.

comparable structures.<sup>31</sup> In addition, the occurrence of the band at 1234 cm<sup>-1</sup> was most likely caused by a C–O stretch of a carboxylic acid. Nyquist and Potts<sup>32</sup> reported for asymmetric O–C–O stretches in proximity of an aromatic system values between 1211 and 1248 cm<sup>-1</sup> which was also in accordance to Silverstein, Bassler and Morrill.<sup>30</sup> Furthermore, Nyquist and Potts reported the existence of out-of-plane skeletal deformations at ~800 cm<sup>-1</sup>, which we correlated to the rising peak at 758 cm<sup>-1</sup>.<sup>32</sup>

Under both, nitrogen and carbon dioxide, conditions a broad band at 3350 cm<sup>-1</sup> from O–H bonds was appearing which did not allow differentiation between the phenolic and carboxylic O–H bond. Besides occurring of a C–O band from the carboxylic acid also the appearance of a C=O band would be expected. Due to the high degree of dissolving during the experiment we assumed this evolving feature to be overlapping with the disappearing C=O of the anthraquinone and other IR features in this region (according to Fig. 6).

Besides the different features of the evolving C<sub>arom</sub>–O under N<sub>2</sub> and CO<sub>2</sub> and the rise of bands at 1234 cm<sup>-1</sup> and 758 cm<sup>-1</sup> from the carboxylic acid underlined the formation of a new



species upon electrochemical reduction of anthraquinone under CO<sub>2</sub> saturated conditions.

In addition to investigations about the structural changes upon the carbon dioxide capture also the quantification of the CO<sub>2</sub> capture process was studied. Assuming the possible uptake of 2 moles CO<sub>2</sub> per anthraquinone molecule resulted in a theoretical uptake capacity of 9.6 mmol<sub>CO<sub>2</sub></sub> g<sub>AQ</sub><sup>-1</sup>. Electrochemical capture and release experiments in triplicates resulted in an average experimental uptake capacity of 5.9 mmol<sub>CO<sub>2</sub></sub> g<sub>AQ</sub><sup>-1</sup>, which referred to an efficiency of 61% (it was assumed that the detected and released amount was equal to the captured amount). As the efficiency was above 50% the assumption of capturing two moles CO<sub>2</sub> per molecule anthraquinone in some parts of the electrode seemed to be plausible. This uptake capacity value was higher than the compounds reported previously by our group<sup>18,19</sup> for electrochemical capture and release and comparable to the industrially-used capturing agent monoethanolamine.<sup>8</sup> Those good capture and release features could be explained by a theory made-up in 1993 by DuBois *et al.*<sup>14</sup> As the binding energy for CO<sub>2</sub> could be related to the  $E_{1/2}$  of the quinone, a half-wave potential of  $-0.5$  to  $-0.7$  V vs. SCE was found to be optimum.<sup>14</sup> Re-calculating the reduction of AQ resulted in a similar potential of  $-0.84$  V vs. SCE.

## 4. Conclusions

In summary, we showed that the simple molecule anthraquinone is able to capture and release CO<sub>2</sub> reversibly upon electrochemical reduction and re-oxidation exhibiting a high uptake capacity of 5.9 mmol<sub>CO<sub>2</sub></sub> g<sub>AQ</sub><sup>-1</sup>. Although the material is dissolving over repetitive cycles under N<sub>2</sub> conditions, it is relatively stable under CO<sub>2</sub> upon formation of a carbonate-like structure. Experiments under CO<sub>2</sub> at constant potential of  $-1.2$  V for 60 minutes as well as for 50 CV cycles confirm this stability. To the best of our knowledge anthraquinone, such simple yet industrially significant molecule, is demonstrated for the first time for its capability of reversible heterogeneous electrochemical capture and release of CO<sub>2</sub> in aqueous solutions under ambient pressure and temperature.

If the CO<sub>2</sub> capture and immobilization is successful on an electrode, the same electrode can be also functionalized with catalysts to make the electrochemical reduction of the captured CO<sub>2</sub>. This combination of capture with reduction of CO<sub>2</sub> is our next level of work.

## Conflicts of interest

The authors declare no competing interests.

## Acknowledgements

Authors gratefully acknowledge the funding of from FWF within the framework of Prof. Sariciftci's Wittgenstein Prize (Solare Energie Umwandlung Z222-N19) and the FFG within the project CO<sub>2</sub> TRANSFER (848862). We kindly acknowledge the help of DI Halime Coskun Aljabour for introducing us to sublimation purification of anthraquinone. The help of Prof. Günther Knör

and Dr Mariusz Wolff for conducting UV-vis measurements in their facilities is gratefully acknowledged.

## Notes and references

- 1 M. Aresta, *Carbon Dioxide Recovery and Utilization*, Springer Science+Business Media, Dordrecht, 2003.
- 2 M. Aresta, *Carbon Dioxide as Chemical Feedstock*, WILEY-VCH Verlag GmbH & Co. KGaA, Weinheim, 2010.
- 3 M. Rakowski Dubois and D. L. Dubois, *Acc. Chem. Res.*, 2009, **42**, 1974–1982.
- 4 J. Ma, N. Sun, X. Zhang, N. Zhao, F. Xiao, W. Wei and Y. Sun, *Catal. Today*, 2009, **148**, 221–231.
- 5 D. H. Apaydin, S. Schlager, E. Portenkirchner and N. S. Sariciftci, *ChemPhysChem*, 2017, **18**, 3094–3116.
- 6 S. Topham, A. Bazzanella, S. Schiebahn, S. Luhr, L. Zhao, A. Otto and D. Stolten, *Ullmann's Encycl. Ind. Chem.*, 2014, pp. 1–43.
- 7 G. T. Rochelle, *Science*, 2009, **325**, 1652–1654.
- 8 T. Supap, R. Idem, P. Tontiwachwuthikul and C. Saiwan, *Int. J. Greenhouse Gas Control*, 2009, **3**, 133–142.
- 9 X. Gui, Z. Tang and W. Fei, *J. Chem. Eng. Data*, 2011, **56**, 2420–2429.
- 10 A. Rehman and S.-J. Park, *Macromol. Res.*, 2017, 1035–1042.
- 11 J. Hu, Y. Liu, J. Liu, C. Gu and D. Wu, *Microporous Mesoporous Mater.*, 2018, **256**, 25–31.
- 12 J. Harada, Y. Sakakibara, A. Kunai and K. Sasaki, *Bull. Chem. Soc. Jpn.*, 1984, **57**, 611–612.
- 13 M. B. Mizen and M. S. Wrighton, *J. Electrochem. Soc.*, 1989, **136**, 941–946.
- 14 D. L. DuBois, A. Miedaner, W. Bell and J. C. Smart, in *Electrochemical and Electrocatalytic Reactions of Carbon Dioxide*, ed. B. P. Sullivan, K. Kristl and H. E. Guard, Elsevier Science Publishers B. V., Amsterdam, 1993, pp. 94–117.
- 15 P. Scovazzo, J. Poshusta, D. DuBois, C. Koval and R. Noble, *J. Electrochem. Soc.*, 2003, **150**, D91.
- 16 B. Gurkan, F. Simeon and T. A. Hatton, *ACS Sustainable Chem. Eng.*, 2015, **3**, 1394–1405.
- 17 W. Yin, A. Grimaud, I. Azcarate, C. Yang and J.-M. Tarascon, *J. Phys. Chem. C*, 2018, **122**, 6546–6554.
- 18 D. H. Apaydin, E. D. Głowacki, E. Portenkirchner and N. S. Sariciftci, *Angew. Chem., Int. Ed.*, 2014, **53**, 6819–6822.
- 19 D. H. Apaydin, M. Gora, E. Portenkirchner, K. T. Oppelt, H. Neugebauer, M. Jakesova, E. D. Głowacki, J. Kunze-Liebhäuser, M. Zagorska, J. Mieczkowski and N. S. Sariciftci, *ACS Appl. Mater. Interfaces*, 2017, **9**, 12919–12923.
- 20 H. Ishida, T. Ohba, T. Yamaguchi and K. Ohkubo, *Chem. Lett.*, 1994, **23**, 905–908.
- 21 R. Ranjan, J. Olson, P. Singh, E. D. Lorange, D. A. Buttry and I. R. Gould, *J. Phys. Chem. Lett.*, 2015, **6**, 4943–4946.
- 22 P. Singh, J. H. Rheinhardt, J. Z. Olson, P. Tarakeshwar, V. Mujica and D. A. Buttry, *J. Am. Chem. Soc.*, 2017, **139**, 1033–1036.
- 23 C. Liu and K. Landskron, *Chem. Commun.*, 2017, **53**, 3661–3664.



- 24 J. Revenga, F. Rodríguez and J. Tijero, *J. Electrochem. Soc.*, 1994, **141**, 330–333.
- 25 A. Babaei, P. A. Connor, A. J. McQuillan and S. Umaphathy, *J. Chem. Educ.*, 1997, **74**, 1200–1204.
- 26 M. Shamsipur, B. Hemmateenejad, A. Babaei and L. Faraj-Sharabiani, *J. Electroanal. Chem.*, 2004, **570**, 227–234.
- 27 M. Jakesova, D. H. Apaydin, M. Sytnyk, K. T. Oppelt, W. Heiss, N. S. Sariciftci and E. D. Glowacki, *Adv. Funct. Mater.*, 2016, **26**, 5248–5254.
- 28 J. Danziger, N. R. Armstrong and J. P. Dodelet, *Chem. Mater.*, 1991, **3**, 812–820.
- 29 National Institute of Advanced Industrial Science and Technology, <http://sdfs.db.aist.go.jp>, accessed 21 December 2017.
- 30 R. M. Silverstein, G. C. Bassler and T. C. Morrill, *Spectrometric identification of organic compounds*, New York, 5th edn, 1991.
- 31 T. R. Criswell and B. H. Klanderma, *J. Org. Chem.*, 1974, **39**, 770–774.
- 32 R. A. Nyquist and W. J. Potts, *Spectrochim. Acta*, 1961, **17**, 679–697.

